THE DERIVATION OF A CO_2 FUGACITY CLIMATOLOGY FROM SOCAT'S GLOBAL IN SITU DATA

L. M. Goddijn-Murphy [1], D. K. Woolf [2], P. E. Land [3], J. D. Shutler [3]

[1] ERI, University of the Highlands and Islands, Ormlie Road, Thurso, UK, Email:Lonneke.goddijn-murphy@uhi.ac.uk
[2] Heriot-Watt University, Stromness, UK
[3] Plymouth Marine Laboratory, Prospect Place, Plymouth, UK

ABSTRACT

The Surface Ocean CO_2 Atlas (SOCAT) has made millions of global underway sea surface measurements of CO_2 publicly available, all in a uniform format and presented as fugacity, f_{CO2}. However, these f_{CO2} values are valid strictly only for the instantaneous temperature at measurement and are not ideal for climatology. We recomputed these f_{CO2} values for the measurement month to be applicable to climatological sea surface temperatures, extrapolated to reference year 2010. The data were then spatially interpolated on a 1°×1° grid of the global oceans to produce 12 monthly f_{CO2} distributions. Our climatology data will be shared with the science community.

1. THE SOCAT DATABASE

1.1. Introduction

The SOCAT database contains millions of surface ocean CO_2 measurements in all ocean areas spanning four decades. All data are put in a uniform format while clearly defined criteria are applied in their quality control. SOCAT has been made possible through the cooperation (data collection and quality control) of the international marine carbon science community. The history and organisation of SOCAT is described in [1]. SOCAT version 1.5 includes 6.3 million measurements from 1968 to 2007 and was made publicly available in September 2011 http://www.socat.info/SOCATv1/ .

SOCAT data is presented as three types of data products: individual cruise files, gridded products and merged synthesis data files. For our study we used the latter and we downloaded the individual regional synthesis files from http://cdiac.ornl.gov/ftp/oceans/SOCATv1.5/. The content of these files (parameter names, units and descriptions) are described in [1]. The data can be displayed online in the Cruise Data Viewer (Fig.1) and downloaded in text format.

1.2. The SOCAT computation of CO_2 fugacity in seawater

The collected CO_2 concentrations were expressed as mole fraction, partial pressure or fugacity of CO_2; SOCAT's recalculation was to achieve a uniform

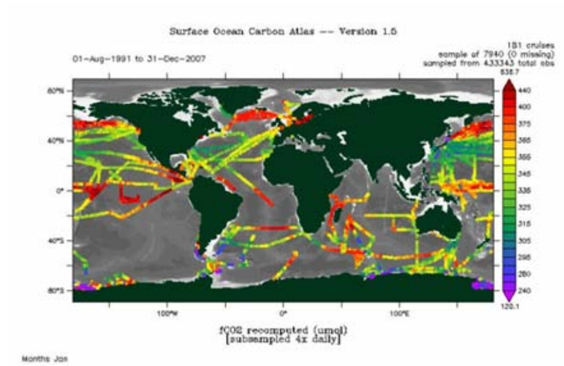

Figure 1. SOCAT CO_2 fugacity (μatm) data shown in the online Cruise Data Viewer for the month January; all data from 1 August 1991 to 31 December 2007.

representation of the CO_2 measurements. All measurements were converted to fugacity in seawater $f_{CO2,is}$ (fCO2_rec) for in situ sea surface temperature, SST (temp), and equilibrator pressure, P_{eq} (Pressure_equi). The parameters in brackets refer to their SOCAT version 1.5 names [1]. The SOCAT fugacity is calculated from $p_{CO2,is}$, partial pressure in seawater corrected for the difference between SST and the temperature at the equilibrator T_{eq} (Temperature_equi), using Eqs. 1&2,

$$p_{co2,is} = p_{co2}(T_{eq}) \exp\{0.0423(SST - T_{eq})\} \quad (1)$$

$$f_{CO2,is} = p_{CO2,is} \exp\left(\frac{[B(CO_2, SST) + 2(1 - X_{CO2,wet}(T_{eq}))^2 \delta(CO_2, SST)] P_{eq}}{R \cdot SST} \right) \quad (2)$$

with $B = B(CO_2, SST)$ and $\delta = \delta(CO_2, SST)$ calculated from

$$B(CO_2, T) = -1636.75 + 12.0408T - 3.27957 \times 10^{-2} T^2 + 3.16528 \times 10^{-5} T^3 \quad (3)$$

$$\delta(CO_2, T) = 57.7 - 0.118T \quad (4)$$

[2]. In Eqs. 1-4 temperatures are in unit K and $X_{CO2,wet}(T_{eq})$ is the wet mole fraction as parts per million (ppm) of CO_2 at equilibrator. Measurement of $p_{CO2}(T_{eq})$, the temperature correction and the necessarily different

Proc. 'ESA Living Planet Symposium 2013', Edinburgh, UK
9–13 September 2013 (ESA SP-722, December 2013)

starting points of the computation are discussed in the following sub sections. Our conversion, from the given f_{CO2} calculated for in situ measurements to f_{CO2} relating to climatological temperatures and atmospheric pressures, is explained in Section 2. The reason for our conversion is that f_{CO2} is highly sensitive to temperature fluctuations and that SST can vary considerably so that an in situ measurement would not give a correct assessment of monthly gridded mean of f_{CO2}. In our conversion a climatological value for P_{eq} is also applied.

1.3. Measurements of $p_{CO2}(T_{eq})$

The method for measurements of p_{CO2} in seawater described by [3] is summarized in the following. On board the ship carrier gas is equilibrated with streaming seawater in the headspace of an equilibrator and the concentration of CO_2 in the equilibrated carrier gas is measured. When a dry carrier gas is analysed, seawater $p_{CO2}(T_{eq})$ in the equilibrator chamber is computed using

$$p_{CO2}(T_{eq}) = X_{CO2,dry}(P_{eq} - P_w) \tag{5}$$

where P_{eq} is the pressure at the equilibrator, P_w water vapour pressure at T_{eq} and salinity S, and $X_{CO2,dry}$ the mole fraction of CO_2 in dry air. P_w is calculated with

$$P_w = \exp\left(24.4543 - 67.4509(100/T_{eq}) - 4.8489(\ln(T_{eq}/100) - 0.000544S\right) \tag{6}$$

[4]. When mixing ratios in a wet carrier gas (100% humidity) are determined P_w is set to zero,

$$p_{CO2}(T_{eq}) = X_{CO2,wet}(T_{eq})P_{eq} \tag{7}$$

1.4. Temperature handling

There are different methods to correct for the difference in partial pressure at intake and equilibrator temperature. SOCAT uses the simple Eq. 1; they refer to more complicated methods but disregard these because they require knowledge of the alkalinity and TCO_2 and are not determined for isochemical conditions. Others [e.g., 3] use

$$p_{CO2,is} = p_{CO2}(T_{eq})\exp\left[0.0433(SST - T_{eq}) - 4.35\times10^{-5}(SST^2 - T_{eq}^2)\right] \tag{8}$$

with SST and T_{eq} in °C.

1.5. Starting points of the SOCAT computation

Different measured parameters are available in different records to use as starting point for the SOCAT re-computation of $f_{CO2,is}$ (Table 4 in [1]). Therefore SOCAT applies the following strict guidelines:

(1) recalculate f_{CO2} whenever possible;

(2) order of preference of the starting point is: x_{CO2}, p_{CO2}, f_{CO2};

(3) minimize the use of external data.

The majority of the cases (57.5%) is derived from $X_{CO2,dry}(T_{eq})$. However, in many cases only $f_{CO2,is}$ (8.4%) or $p_{CO2,is}$ (13.8%) was provided so that it is not certain that Eq. 1 was used by the cruise scientists to convert $p_{CO2}(T_{eq})$ to $p_{CO2,is}$. Moreover, if only $f_{CO2,is}$ was reported, but pressure and salinity were not, $f_{CO2,is}$ is not recalculated and $f_{CO2,is}$ is taken as provided. The regional synthesis files only contain recomputed $f_{CO2,is}$ values and don't give direct information about starting points other than which one was used (fCO2_source). However, each record contains a field 'doi', indicating the digital object identifier to a publically accessible online data file in the PANGEA database (http://www.pangaea.de/) where the original measurements before re-computation can be found. The individual cruise data files also contain various x_{CO2}, p_{CO2}, and f_{CO2} data (Table 5 in [1]). Because we wanted to use SOCAT 's uniform database, and not re-create it, we estimated $f_{CO2,cl}$ from the $f_{CO2,is}$ values in the merged synthesis files as explained in Section 2. An estimation of the error in re-computed $f_{CO2,cl}$ due to varying starting points is given in Sections 4.6 & 4.7.

1.6. SOCAT quality control

Basic, primary quality control is carried out during the first stage of converting the data to a common file structure. Whenever outliers and unrealistic values are encountered, the data originator is contacted and this often results in resubmission of corrected version. Bad data are removed from the data file if the data originator cannot be contacted. In version 2 of SOCAT this class of quality control is used to assign quality flags to individual data points, using the conventions of the World Ocean Circulation Experiment (WOCE): flag 2 (good), flag 3 (questionable) or 4 (bad). Only a very small number of WOCE flags 3 and 4, 0.2% [5], are found in the version 1.5 data collection. The WOCE flag is the 'WOCE_flag' parameter in the synthesis files.

SOCAT regional groups have carried out a second quality control by flagging each cruise, giving information on the expected quality of the $f_{CO2,is}$ data [1]. This includes checks of the sampling positions and time, atmospheric pressures, salinity, intake and equilibrator temperatures, as well as recommended f_{CO2} data, and where possible a comparison with other data from the same region. The criteria for the cruise flags are listed in Table 6 in [1]. The data quality decreases as the cruise flag ranges from A, B, C, D, S. Only cruises flagged A, B, C and D are included in the SOCAT products. Cruise flags A and B ascertain SOP (Standard Operating Procedures) criteria were used [1], resulting in an f_{CO2} accuracy of 2 µatm or better. If a large number (> 50, as a guideline) of non-acceptable data were found, the data file was suspended while the data contributor was invited to submit a suitably revised version of the data. If it was not possible to establish contact with the data originator, or if the number of unacceptable data was sufficiently small (typically less than 50), WOCE flags 3 (questionable) or 4 (bad) were assigned to each unacceptable f_{CO2} recommended value. However, while 0.2% of the WOCE flags were assessed flags 3 and 4 during version 1 quality control, virtually all such flags were unintentionally reset to flag 2 in the version 1 data products [1,5]. The WOCE flags 3 and 4 assigned during version 1 quality control are applied in the SOCAT version 2 products. Cruise flag is not a parameter in the downloadable data files but they can be selected in the online cruise data viewer (QC Flag).

2. OUR RECOMPUTATION FOR CLIMATOLOGICAL FUGACITY IN THE YEAR 2010

2.1. Inversion: Conversion of $f_{CO2,is}$ to $p_{CO2}(T_{eq})$

We used Eqs. 1&8 to calculate $f_{CO2,cl}$. Because mole fraction $x_{CO2,is}$, and partial pressures $p_{CO2,is}$ and $p_{CO2}(T_{eq})$ are not given in the SOCAT regional synthesis files, the first step was to estimate the original measurement of $p_{CO2}(T_{eq})$ from SOCAT's recomputed $f_{CO2,is}$. First $p_{CO2,is}$ was derived from $f_{CO2,is}$ by inverting Eq. 2:

$$p_{CO2,is} = f_{CO2,is} \exp\left(- \frac{\left[B + 2(1 - X_{CO2,wet}(T_{eq}))^2 \delta\right] P_{eq}}{R \cdot SST} \right) \tag{9}$$

with $B = B(CO_2, SST)$, $\delta = \delta(CO_2, SST)$ from Eqs. 3&4. Defining $X_{CO2,wet}(T_{eq})$ by Eq. 7 and writing $p_{CO2}(T_{eq})$ in terms of $p_{CO2,is}$ (Eq. 1), Eq. 9 gives

$$p_{CO2,is} = f_{CO2,is} \exp\left(- \frac{\left[B + 2\left(1 - \frac{p_{CO2,is} \exp(-0.0423(SST - T_{eq}))}{P_{eq}} \right)^2 \delta \right] P_{eq}}{R \cdot SST} \right) \tag{10}$$

Eq. 10 was solved with an iterative calculation

$$\left[p_{CO2,is}\right]_{n+1} = f_{CO2,is} \exp\left(g(\left[p_{CO2,is}\right]_n, SST, T_{eq}, P_{eq})\right) \tag{11}$$

(g is the function describing the exponent). In the first iteration the initial guess of $[p_{CO2,is}]_1$ was $f_{CO2,is}$ and the result $[p_{CO2,is}]_2$ was put back in the right hand side of Eq. 11. This step was repeated until $|[p_{CO2,is}]_N - [p_{CO2,is}]_{N-1} < 2^{-52}$. Using Eq. 1 we could then estimate the original $p_{CO2}(T_{eq})$ from $p_{CO2,is}$.

$$p_{CO2}(T_{eq}) = p_{CO2,is} \exp\left(-0.0423(SST - T_{eq})\right) \tag{12}$$

2.2. Conversion of $p_{CO2}(T_{eq})$ to $f_{CO2,cl}$ in the year 2010

The next step was to convert partial pressure at equilibrator temperature to partial pressure at climatological SST. We used global 1° × 1° skin SST data from the Advanced Along Track Scanning Radiometer (AATSR). For air-sea flux calculations a climatological subskin SST should be used [6]. Subskin SST is slightly cooler than SST nearer the surface, and to account for the cooling effect on the sea surface a value of 0.14 was added ($T_{cl} = SST_{AATSR} + 0.14$) [7]. Because AATSR data were available from August 1991 we converted SOCAT data from then onwards, which accounts for 98.6% of all SOCAT version 1.5 data. Following [3] we used Eq. 8 to correct for the difference between climatological and equilibrator temperature.

Next, $p_{CO2,cl}$ was extrapolated to the year 2010 using the mean rate of change of 1.5 ± 0.3 µatm y^{-1} [3]. Finally $f_{CO2,cl}$ was derived using Eq. 2 with SST = T_{cl} and $P_{eq,cl}$ estimated from a climatological value of atmospheric pressure, $P_{atm,cl}$. For $P_{atm,cl}$ we used sea level pressure estimated as closest grid value from 6 hourly NCEP/NCAR given in SOCAT's merged synthesis files (ncep_slp). To account for the overpressure that is normally maintained inside a ship 3 hPa was added ($P_{eq,cl} = P_{atm,cl}$ + 3 hPa) [3].

Note that we recomputed SOCAT's $f_{CO2,is}$ for climatological SST and atmospheric pressure, but not for climatological salinity. However, if in situ salinity was not provided by the investigator, SOCAT used a climatological sea surface salinity from the World Ocean Atlas 2005 (woa_sss) for their computation of $f_{CO2,is}$.

2.3. Missing values

We dealt with missing variables in analogy with [4]:

1. we only used records with WOCE_flag = 2;
2. we used only records with valid values for $f_{CO2,is}$ and SST;
3. if T_{eq} was invalid, we used SST;
4. if P was invalid, we used ncep_slp ;
5. if P_{eq} was invalid, we used P + 3 hPa.

3. HORIZONTAL EXTRAPOLATION USING ORDINARY BLOCK KRIGING

The data were grouped by month and for each month $f_{CO2,cl}$ and $p_{CO2,cl}$ estimated for 2010 were averaged over 1° × 1° squares. For the spatial interpolation of these gridded data on a mask map of the global oceans we used gstat, an open source computer code for multivariable geostatistical modelling, prediction and simulation (gstat home page: http://www.gstat.org/). For each month we modelled the variogram for the $f_{CO2,cl}$

data [8]. The variogram best fitted a combination of a nugget and a spherical model, aNug() + b Sph(c). The fitted variogram model was applied in the kriging of both $f_{CO2,cl}$ and $p_{CO2,cl}$. We performed local ordinary block kriging on a mask map of the global oceans with min=4, max=20, and radius=60. Thus, after selecting all data points at (euclidian) distances from the prediction location less or equal to 60, the 20 closest were chosen when more than 20 were found and a missing value was generated if less than 4 points were found. The data were smoothed by averaging over square shaped blocks of size: dx=5, dy=5. These results were compared with the results using different kriging options (Table 1, Section 4.3).

4. RESULTS

4.1. Monthly global maps

After the Oceanflux Greenhouse Gases (GHG) project finishes at the end of 2013, the global distribution data will be made available in 12 monthly netCDF-3 files through the project website http://www.oceanflux-ghg.org/Products/OceanFlux-data/Monthly-composite-datasets (Currently registered users have limited access). These files contain $f_{CO2,cl}$, $p_{CO2,cl}$, their spatial interpolation errors, SST_{AATSR}, and atmospheric fraction of CO_2 in dry air (parts per million) from the GlobalView CO_2 database (http://www.esrl.noaa.gov/gmd/ccgg/globalview/co2/co2_intro.html), for the year 2010, all on a 1° × 1° grid. The $p_{CO2,cl}$ values are given for those who prefer to use partial pressure, levels are slightly higher (less than 2 µatm) than $f_{CO2,cl}$. A range of possible errors need to be considered when interpreting the final twelve monthly maps (Figs. A1&A2). These are discussed in the following six Sections.

4.2. Spatial interpolation errors

The standard deviations of the applied kriging were calculated by taking the square root of the variance values produced by gstat [8]. The $f_{CO2,cl}$ kriging uncertainties mapped for all months are illustrated in Fig. A2. These errors could be significant, exceeding 50 µatm in places, and were the lowest (< 10 µatm) in the North Atlantic and North Pacific where the most measurements were available. The month April showed the highest errors, this could be a consequence of the variogram range, c, being the smallest. Our variogram model did not fit November data well, as the semivariance was almost independent of distance; this appeared to be reflected in low standard deviations.

4.3. Comparison of different kriging approaches

The global monthly, gridded values were spatially interpolated using ordinary block kriging with a range of sensible kriging parameters (Table 1). The standard deviation of the mean over the different kriging results (Fig. 2) was less than 5 µatm in most places, with higher values seen near the coasts, Arctic, and the western Tropical Pacific and Southern Ocean. These standard deviations were considerably smaller than those generated by kriging itself (Fig. A2).

Table 1. The different kriging options that were applied to $fCO_{2,\,cl}$; min, max, radius, dx and dy as in Section 3.

min	*max*	*radius*	*dx*	*dy*
4	20	60	5	5
4	20	40	5	5
4	20	100	5	5
4	20	60	1	1
4	20	60	10	10
4	10	60	5	5
4	40	60	5	5
2	20	60	5	5
10	20	60	5	5

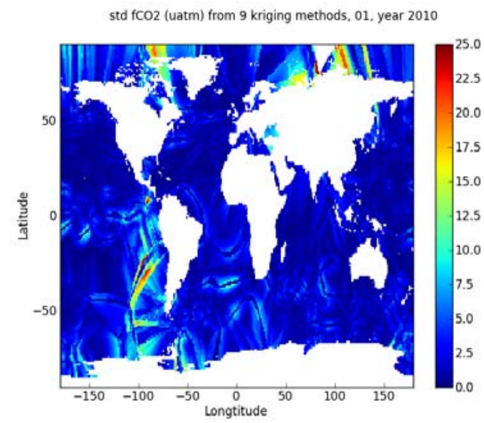

Figure 2. Standard deviations of the mean over the different kriging results of fCO2,cl for range of options (Table 1); on a 0 to 25 µatm scale.

4.4. Were some cruises more important than others?

The bootstrap method creates synthetic sets of data by random resampling from the original data with replacement. We bootstrapped the $fCO_{2,cl}$ data by cruise ID to test if some cruises dominated our results. Re-computing and kriging these datasets showed that significant variation of up to around 50 µatm between the 10 bootstrapped datasets could occur in regions of few cruises (Fig. 3). It was therefore likely that certain cruises were indeed more important than others.

4.5. Temporal extrapolation error

The rate of change in $p_{CO2,cl}$ has an estimated precision of ± 0.3 µatm y^{-1} [3], it can be shown that $\Delta f_{CO2,cl} = \Delta p_{CO2,cl}$. The error in $f_{CO2,cl}$ in 2010 due to uncertainty of the $p_{CO2,cl}$ trend was therefore estimated as (2010-year)×0.3 µatm y^{-1}, ranging between 0.9 – 5.73 µatm. These errors for the month of January are shown in Fig. 4.

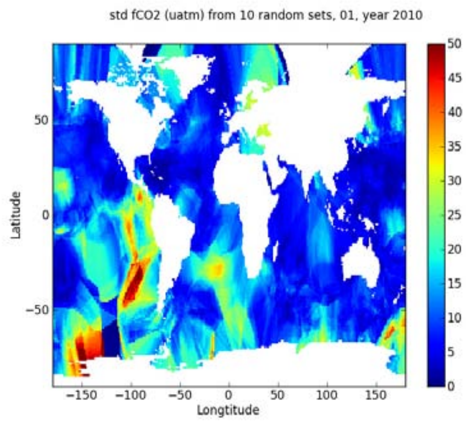

Figure 3. Standard deviations of the mean over 10 bootstrapped datasets of fCO2,cl estimated for January 2010; on a 0 to 50 µatm scale (kriging as in Section 3).

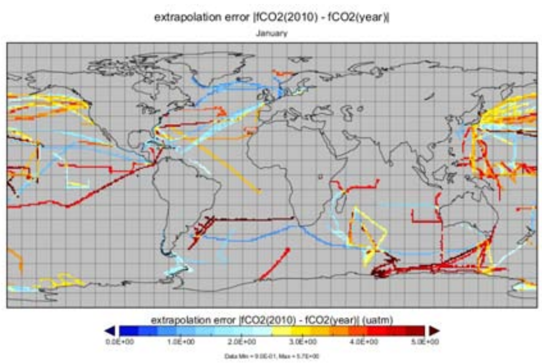

Figure 4. Caluclated progression of the 'temporal extrapolation error' in $f_{CO2,cl}$ estimated for January 2010; on a 0 to 5µatm scale.

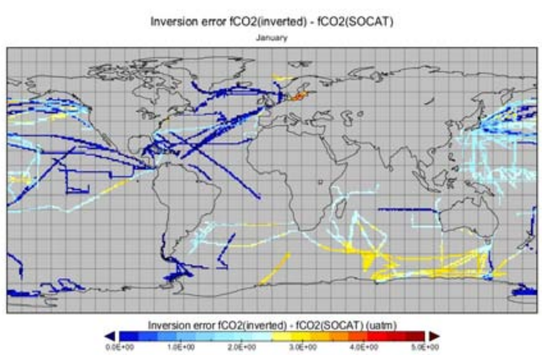

Figure 5. Calculated 'inversion error' in $f_{CO2,cl}$ estimated for January 2010; on a 0 to 5µatm scale.

4.6. Inversion error

Our conversion of $f_{CO2,is}$ to $p_{CO2}(T_{eq})$ could introduce an error if the data was not based on x_{CO2} analysis (cruise flags not A or B), but on f_{CO2} calculated from a spectrophotometer, or if the investigator only provided $f_{CO2,is}$ or $p_{CO2,is}$ and did not use Eq. 1 to correct for the temperature difference. This error was assessed by calculating the conversion from $f_{CO2,is}$ to $f_{CO2,cl}$ using SST and P_{eq} instead of T_{cl} and $P_{eq,cl}$ and omit the extrapolation of $p_{CO2,cl}$ to 2010. This conversion would ideally produce the original SOCAT $f_{CO2,is}$ value. A difference between $f_{CO2,is}$ and '$f_{CO2,cl=is}$' implied that our re-computation differed from the one applied by SOCAT or the investigator and we called this difference 'inversion error'. These errors appeared to be relatively small and neglible in most places (Fig. 5).

4.7. Missing values

Missing values did not always propagate into an inversion error because we made an effort to handle the missing values conform SOCAT [4], but missing values could introduce significant systematic errors. It is difficult to estimate the size of these kinds of errors, but Fig. 6 shows the proportion of missing values for January to give an idea about how many data could be affected.

The $f_{CO2,cl}$ calculations were most sensitive to temperature. If T_{eq} was not provided we used in situ SST, so an inversion error would be near zero. However, in this case $p_{CO2,is}$ was then the starting point of our conversion instead of $p_{CO2}(T_{eq})$, which could lead to significant systematic $f_{CO2,cl}$ errors. If salinity or pressure were missing, SOCAT used climatological values for their conversion, reducing systematic $f_{CO2,cl}$ errors for these data points.

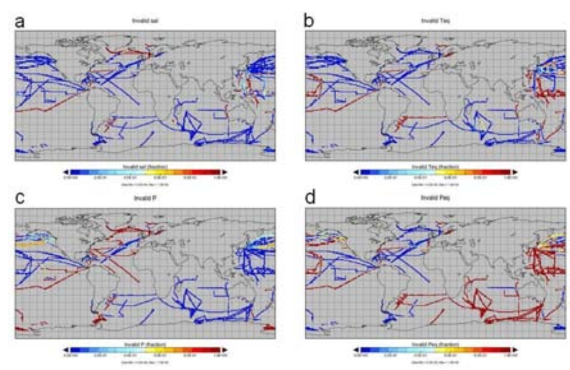

Figure 6. Fractions of $f_{CO2,cl}$ estimated for January 2010, calculated with missing value (a) Salinity, (b) T_{eq}, (c) P, and (d) P_{eq}; on a 0 to 1 scale.

We also reproduced our $f_{CO2,cl}$ distribution maps using only data points with valid values for T_{eq} (Fig. 7). These maps showed missing high $f_{CO2,cl}$ locations. This dataset will also be provided after the Oceanflux GHG project is finished on the project website.

5. SOCAT VERSION 2

Recently, on 4 June 2013, the updated database SOCAT version 2 was released containing 10.1 million surface water f_{CO2} values [5]. The added data are from cruises during the years 2008 to 2011, from the Arctic, and previously unpublished data from earlier cruises; also the quality control is improved. The WOCE flags 3 and 4 that were unintentionally reset to flag 2 (good) in the SOCAT version 1 data products are re-assigned in the version 2 products. The addition of SOCAT data points and the omission of bad and questionable data gave generally smoother global distributions (Fig. 8) and smaller kriging errors (not shown). Our re-processed SOCAT version 2 data for climatology will also be made available after the Oceanflux GHG project ends.

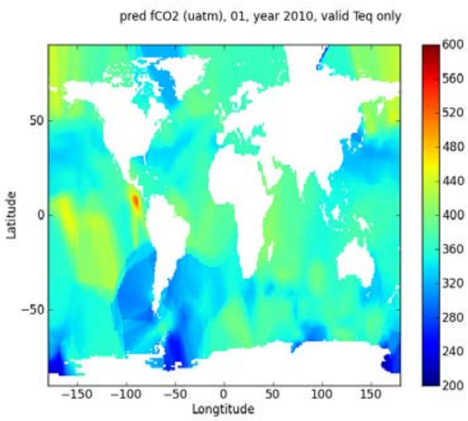

Figure 7. As Fig. A1, January, but using only data points with valid T_{eq}.

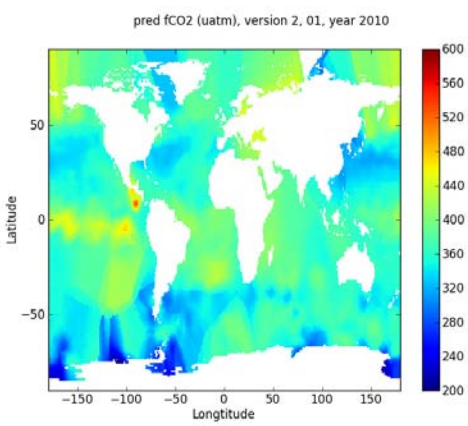

Figure 8. As Fig. A1, January, but using SOCAT version 2 data.

6. CONCLUSION

SOCAT f_{CO2} values, recomputed for climatological temperature and pressure and interpolated to a global 1°×1° grid, will be made available together with other climatological data necessary to calculate global oceanic CO_2 fluxes. We identified possible errors, it is difficult to add these up because they have different origins (measurement, conversion, and extrapolation) but some areas showed higher errors of all kinds than others. The data quality in the North Atlantic and North Pacific appeared to be superior. Our dataset based on SOCAT version 2 is mostly similar to the one based on version 1.5, but if it is used to focus on outliers version 2 should be used. For future SOCAT versions it would be ideal if the climatological values of f_{CO2} were directly calculated (Eq. 8) and included, so to avoid the need for the inversion step.

ACKNOWLEDGEMENTS

This research is a contribution of the National Centre for Earth Observation, a NERC Collaborative Centre and was supported by the European Space Agency (ESA) Support to Science Element (STSE) project OceanFlux Greenhouse Gases (contract number: 4000104762/11/I-AM). We appreciate the use of the SOCAT data, made available by SOCAT investigators, regional group leaders, quality controllers and data providers.

REFERENCES

1. Pfeil, B., Olsen, A. & Bakker, D. C. E. et al. (2013), A uniform, quality controlled Surce Ocean CO_2 Atlas (SOCAT), *Earth Syst. Sci. Data*, 5, 125-143.

2. Weiss, R. F. (1974), Carbon dioxide in water and seawater: the solubility of a non-ideal gas, *Mar. Chem., 2*, 203-215.

3. Takahashi, T. et al. (2009), Climatological mean and decadal change in surface ocean pCO_2, and net sea–air CO2 flux over the global oceans, *Deep-Sea Res. II, 56*, 554-577.

4. Pfeil, B. & Olsen, A. (2009), A uniform format surface fCO_2 database, *available at: http://www.socat.info/publications.html (last access: 4 June 2012)*, 1-9.

5. Bakker, D. C. E., Pfeil, B. & Smith, K. et al. (2013), An update to the Surface Ocean CO_2 Atlas SOCAT version 2), submitted to *Earth Syst. Sci. Data.*

6. Woolf, D. K., Land, P. E., Shutler, J. D. & Goddijn-Murphy, L. M. (2012), Thermal and haline effects on the calculation of air-sea CO_2 fluxes revisited, *Biogeosciences Discuss., 9*, 16381-16417.

7. Donlon, C. J., Minnett, P., Gentemann, C. L., Barton, I. J., Ward, B., Murray, J. & Nightingale, P. D. (2002), Towards operational validation of satellite sea surface skin temperature measurements for climate research, *J. Climate, 15*, 353-369.

8. Pebesma, E. J. (1999), Gstat's user manual, *available at: http://www.gstat.org/gstat.pdf (last access: 27 February 2013)*, 1-100.

1. Appendix A

A.1. Monthly global distributions of $f_{CO2,cl}$ in 2010

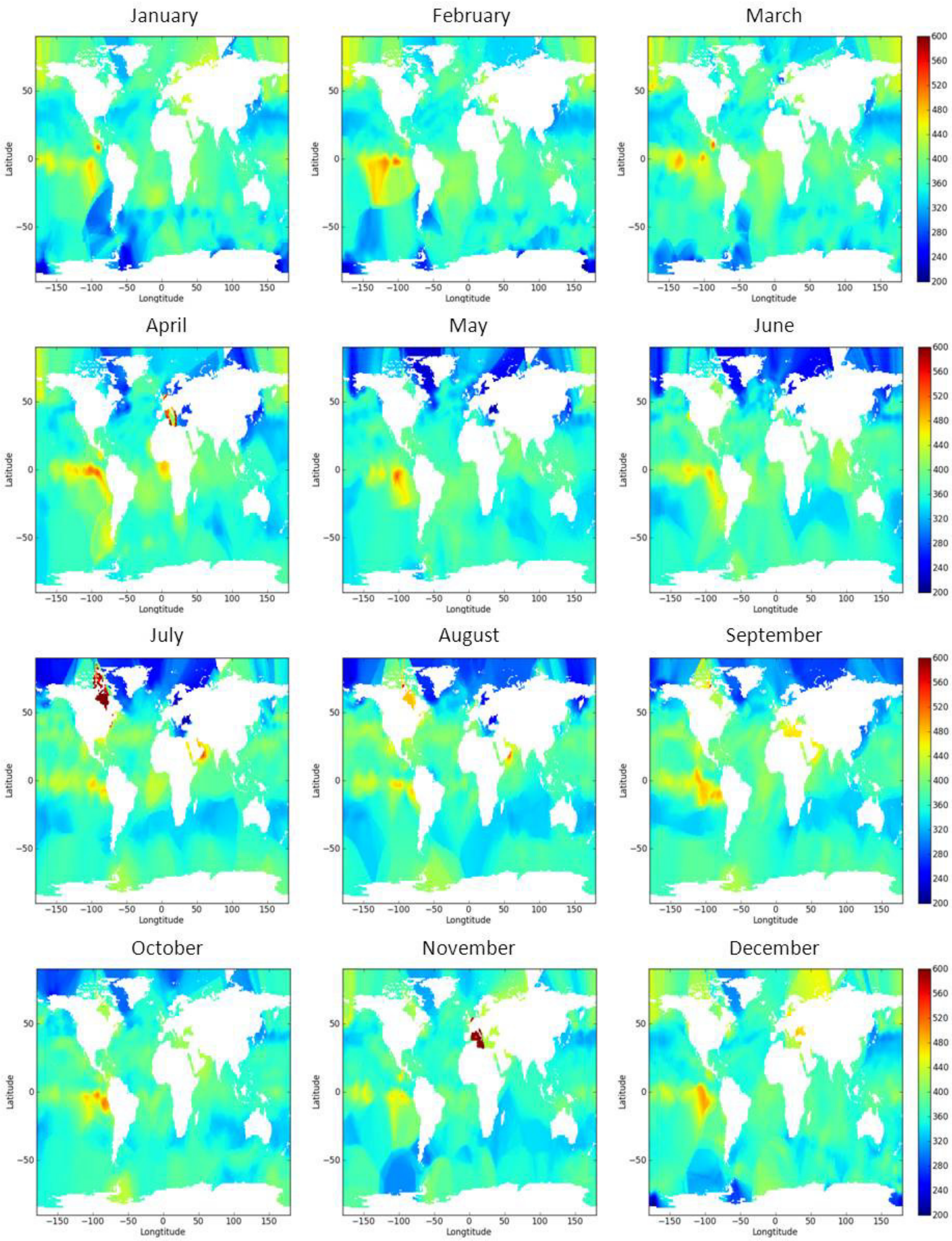

Figure A1. Monthly $f_{CO2,cl}$ values in the global oceans estimated for 2010 on a 200-600 µatm scale; data were interpolated to a 1°×1° grid using ordinary block kriging with min=4, max=20, radius=60 and block size 5x5.

A.2 Spatial interpolation errors in estimations of $f_{CO2,cl}$ in 2010

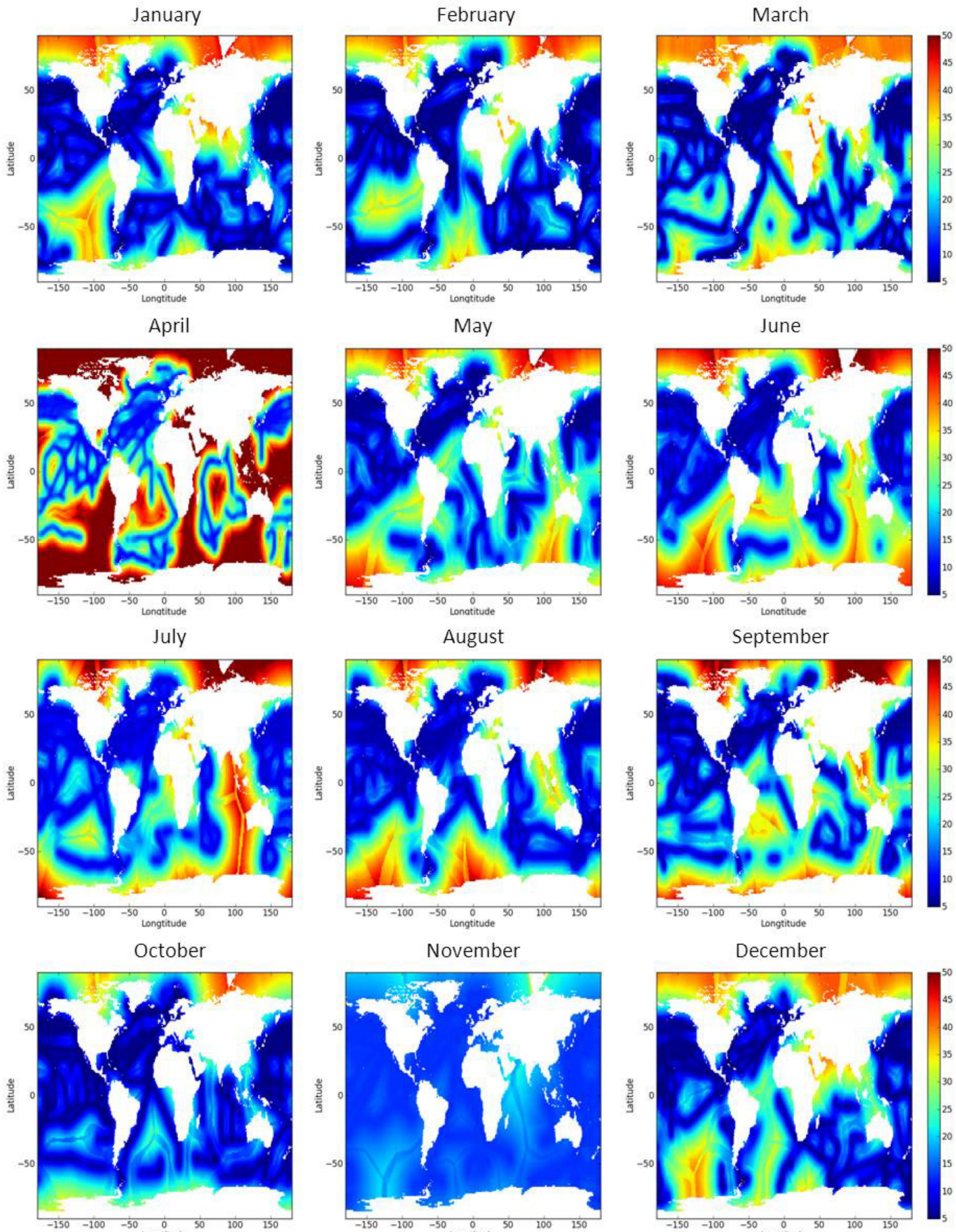

Figure A2. Standard deviation in $f_{CO2,cl}$ estimated for 2010 associated with the ordinary block kriging results shown in Fig. A.1; on a 5 to 50 µatm scale.